Investigation of Mathematical Models of Otolith Organs for Human Centered Motion Cueing Algorithms

Robert J. Telban*
Frank M. Cardullo†
Liwen Guo‡
State University of New York
Binghamton, New York

Abstract

The authors, as part of their work in human centered motion cueing algorithms, conducted research in the area of mathematical modeling of the otolith organs, the sensors of specific force. The purpose of this study was to develop a model that is consistent with both experimental and theoretical analyses that can be readily implemented into a motion cueing algorithm.

The authors reviewed several existing models that characterize the specific force response dynamics. Experimental research on the ocular torsion response of human subjects[8] resulted in a second-order model with a first-order lead component, with a short time constant of 0.66 seconds. From this model and physiological knowledge, a first-order lead-lag model of the otolith afferent dynamics was estimated[2]. A second-order lumped parameter model for the otolith displacement as a function of the specific force stimulus was derived[11], revealing a short time constant of 0.0002 seconds. Physiological experiments measuring the afferent response[6] resulted in an otolith mechanics time constant of 0.016 seconds. Based upon these results found in the literature, the authors synthesized a new otolith model.

The physiological experiments also resulted in models for both regular and irregular units containing a fractional exponent term in the transfer function. The authors derived time responses for these models using fractional calculus with a series approximation. The responses from these models are compared to the response obtained from the proposed model. This comparison illustrates that the proposed model is a reasonable approximation to the more complex physiological models.

Introduction

The otolith organs are located in the inner ear and provide linear motion sensation in humans and mammals. These organs are responsive to specific force, the gravitoinertial reaction force per unit mass, which is defined to be $\underline{f}_X = \underline{g}_X - \underline{a}_X$,[1,2] where $\underline{g}_X$ is the local gravitational force vector, and $\underline{a}_X$ is the acceleration of the head with respect to a body-fixed reference frame. Therefore, the otoliths respond to both linear acceleration of the head and tilting of the head with respect to the gravity vector. However, the otoliths cannot discriminate between acceleration and tilt, requiring additional sensory information to resolve this ambiguity. There are two otolith organs, the utricle and saccule, in each inner ear. The utricle primarily senses motion in the longitudinal and lateral planes, while the saccule primarily senses motion in the vertical plane.

The orientation of the otolith organs with respect to a body-fixed reference frame located on the head is shown in Figure 1. The otolith reference frame is fixed to the head; thus motion in this frame is relative to the head. The x-z plane of the otolith reference frame is tilted upward from the x-axis by about 20 degrees.[3] The utricle is oriented along the x-axis and the saccule is oriented along the z-axis in the otolith reference frame.

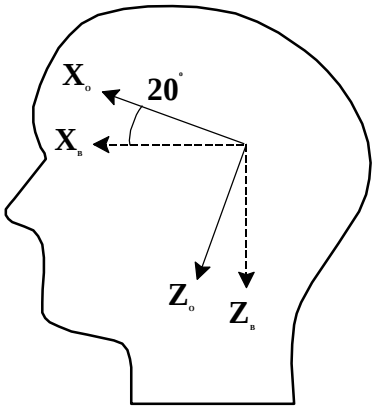

Figure 1. Orientation of the Otolith Organs and Body-Fixed Reference Frame.

---

* PhD Candidate, Department of Mechanical Engineering, Student Member AIAA
† Associate Professor, Department of Mechanical Engineering, Associate Fellow AIAA
‡ PhD Student, Department of Mechanical Engineering.

Physiological Description of the Otoliths

The otolith organs consist of a two-layer structure known as the otolithic membrane that is attached to a base containing sensory cells. The otolithic membrane is composed of an upper layer, the otoconial layer, and a lower layer, the gelatinous layer. A fluid known as endolymph is in contact with the upper surface of the otoconial layer. The otoconial layer consists of calcium carbonate crystals embedded in a gelatinous material that rests on a less dense and extremely deformable gelatinous layer. This gelatinous layer is in turn attached to the sensory cell base known as the macula that is incorporated into the membranous tissue walls of the inner ear. The macula is rigidly attached to the skull and therefore moves with the head.

There are two types of sensory cells located in the macula. The Type I cells are enclosed in a nerve chalice and are innervated by nerve fibers with a large diameter. The Type II cells are cylindrical and are innervated by fibers with a small diameter. Fernandez and Goldberg[4] report that cells in the outer (peripheral) otolith region are primarily Type II cells and cells in the central (striolar) region are primarily Type I cells. Both types of cells have a series of small hairs that penetrate the lower portion of the gelatinous layer. Each hair cell has about 70 stereocilia and one kinocilium with the stereocilia graded in length toward the kinocilium.

The resulting displacement of the otolithic membrane due to forward linear acceleration is illustrated in Figure 2. The arrows in the figure show the direction of the specific force acting upon the head. With a forward acceleration or backward tilting of the head the denser otoliths tend to lag behind the macula, with the relative motion resulting in deforming the gelatinous and otoconial layers in shear. When the shear deformation is in the direction of the kinocilium, the cell will be excited, whereas when the deformation is in the opposite direction, the cell will be inhibited. The directions of the maximum excitation and inhibition of a hair cell are defined by its polarization axis. In each macula, the striola separates oppositely polarized regions. For each position due to translational movement, some cells will be maximally excited, while others will be maximally inhibited.

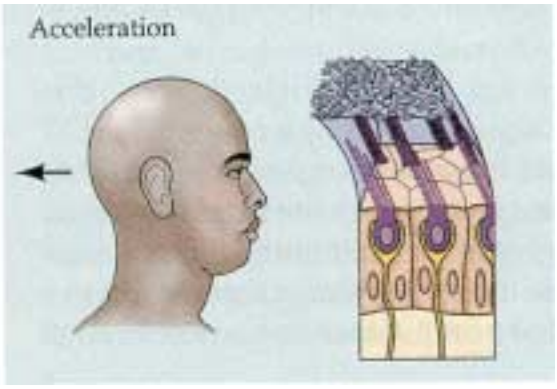

Figure 2. Displacement of the Otolithic Membrane due to a Forward Acceleration[5].

The axes of maximum and minimum response of a given afferent neuron are defined by the corresponding polarization axis of the hair cells that it innervates. The linear polarization of an afferent neuron strongly suggests that the hair cells that the neuron innervates have polarization axes that are oriented in the same direction.[3,4] The response of a neuron is the afferent firing rate (AFR), measured in impulses per second (IPS).

Fernandez and Goldberg[6] identified two types of neurons that are characterized by their variance or regularity of discharge, hereafter referred to as regular and irregular units. From a sample population of units, they identified a ratio of regular to irregular units to be approximately three to one.

Physiologically Based Models of Perceived Response

Zacharias[7] reported that Meiry (1965) first investigated subjective responses to linear motion by using a cart to produce longitudinal sinusoidal motion. By measuring the subjective indication of direction, he obtained a transfer function relating perceived velocity $\hat{v}$ to actual velocity v:

$$\frac{\hat{v}(s)}{v(s)} = \frac{K\tau_1 s}{(\tau_1 s + 1)(\tau_2 s + 1)} \tag{1}$$

Where the long time constant τ_1 and short time constant τ_2 are 10 and 0.66 seconds respectively, and the gain K is undetermined since amplitude measurements were not taken. Zacharias[7] then noted that Peters suggested the subjective response measured by Meiry was

perceived acceleration and not perceived velocity, since in response to an acceleration step the model predicted a perceived response that decays to zero with a time constant of 10 seconds.

Young and Meiry[8] noted that the model proposed by Meiry correctly predicted the phase of perceived velocity for lateral oscillation and time to detect motion under constant acceleration, but failed to predict the otoliths' response to sustained tilt angle as indicated by behavioral and physiological data. They noted that the model agreed with dynamic counter-rolling data (of the eye) at high frequencies, but experimental counter-rolling at zero frequency showed a static component of otolith output with no phase lag (the model assumed no static output and at zero frequency approached 90 degrees of lead). They proposed the following revised model of specific force sensation:

$$\frac{\hat{f}(s)}{f(s)} = \frac{1.5\,(s + 0.076)}{(s + 0.19)(s + 1.5)} \qquad (2)$$

which, when rearranged in terms of the time constants, yields

$$\frac{\hat{f}(s)}{f(s)} = \frac{0.4\,(13.2s + 1)}{(5.33s + 1)(0.66s + 1)} \qquad (3)$$

With a smaller long time constant (5.33 seconds) and an additional lead term, they modeled both perceived tilt and acceleration in response to acceleration input. They noted that the model acts as a velocity transducer over the frequency range of 0.19 to 1.5 rad/s, with the transfer function from specific force to perceived tilt or lateral acceleration having a static sensitivity of 0.4.

Analytical Model of Otolith Dynamics

Zacharias[7] noted that a mass-spring-dashpot model of otolith motion could be used to represent the two lag time constants, similar to the torsion-pendulum model for the semicircular canals. Ormsby[2] first developed this model, and Grant, Best, et al[9,10,11,12] later refined the model as part of their theoretical analysis of the otolithic membrane. A lumped parameter model is constructed by considering the forces on the otoconial layer. The differential equation for this model in the x-direction (in the otolith reference frame) is given as[11]

$$-b\dot{x} - kx + m_o g_x + m_{df}\,(a_x - g_x) = m_o a_B \qquad (4)$$

where

m_o = Mass of the displaced otoconial layer
m_{df} = Mass of the displaced fluid (endolymph)
g_x = Component of the gravity vector
b = Viscous damping on the otoconial layer
k = Stiffness of the gelatinous layer
x = Displacement of the otoconial layer with respect to the head
a_x = Acceleration of the head with respect to a body-fixed reference frame
a_B = Acceleration of the otoconial membrane with respect to a body frame

The force term of $m_{df}(a_x - g_x)$ is the buoyant force of the endolymph acting on the otoconial layer, which was neglected by Ormsby[2] in his analysis.

By conservation of volume, the mass of the displaced fluid can be expressed as $m_{df} = (\rho_e / \rho_o)\, m_o$, where ρ_e is the density of the endolymph and ρ_o is the density of the otoconial membrane. Substituting this term into Eqn. (4), and noting that $a_B = a_x + \ddot{x}$, results in

$$\ddot{x} + \frac{b}{m_o}\dot{x} + \frac{k}{m_o}x = \left(1 - \frac{\rho_e}{\rho_o}\right)(g_x - a_x) \qquad (5)$$

Note that the stimulus term $g_x - a_x$ is the specific force component f_x. The term $(1 - \rho_e / \rho_o)$ establishes the system sensitivity or gain to the stimulus terms. For ρ_o greater than ρ_e, a positive g_x or a negative a_x will produce a positive displacement of the otoconial layer. Eqn. (5) can then be written in transfer function form as

$$\frac{x(s)}{f(s)} = \left(1 - \frac{\rho_e}{\rho_o}\right)\frac{1}{\left(s^2 + \frac{B}{m_o}s + \frac{K}{m_o}\right)} \qquad (6)$$

As observed by Young and Meiry[8], the system response is overdamped. For an overdamped system, Eqn. (6) can be rewritten in terms of the long and short time constants as

$$\frac{x(s)}{f(s)} = \left(1 - \frac{\rho_e}{\rho_o}\right) \frac{\tau_1 \tau_2}{(1+\tau_1 s)(1+\tau_2 s)} \qquad (7)$$

where for the otoliths, τ_1 ? τ_2, and therefore the two time constants can be related to the lumped parameters as $\tau_1 = m_o / k$ and $\tau_2 = m_o / b$.

In determining the value of the short time constant τ_2, Grant and Best[11] examined the maximum displacement of the otoconial layer in response to a step change in linear velocity. The acceleration for a linear velocity step U is $a_x = -U\delta(t)$, with g_x = 0, where $\delta(t)$ is the unit impulse function. The transient response to Eqn. (7) is then

$$x(t) = U\left(1 - \frac{\rho_o}{\rho_e}\right)\tau_2 (e^{-t/\tau_1} - e^{-t/\tau_2}) \qquad (8)$$

By assuming that the short exponential term in Eqn. (8) has reached zero and the long exponential term remains close to unity, the maximum displacement of the otoconial layer $x_{\max}$ can be approximated as

$$x_{\max} \cong U\left(1 - \frac{\rho_e}{\rho_o}\right)\tau_2 \qquad (9)$$

The theoretical continuum mechanics analysis performed by Grant and Best first indicated that this short time constant τ_2 is 0.002 seconds or less[10]. They later demonstrate[11] that this value turns out to be too large when reasonable values of the maximum otolith displacement are considered. For ρ_o = 2.0 and U = 25 cm/sec (a reasonable value for normal head velocity), Eqn. (9) becomes $x_{max} = 12.5\tau_2$. For τ_2 = 0.002 sec, the maximum displacement of the otolithic membrane results in x_{max} = 250 μm. It is assumed that for shear deformation the maximum displacement should not exceed the thickness of the otoconial layer (25 μm), indicating the short time constant should be one order of magnitude smaller, i.e. τ_2 = 0.0002 s. This indicates that more damping is needed in the lumped parameter model. Grant and Best later show that additional damping can be introduced by inclusion of a viscoelastic gelatinous layer in the continuum mechanics model[12].

Estimated Model of Afferent Dynamics

Ormsby[2] neglected the short time constant τ_2 in Eqn. (7) and after rearranging terms, approximated the otolith mechanical dynamics by

$$\frac{x(s)}{f(s)} = \frac{A}{s + A} \qquad (10)$$

and then proposed a model for the response of the otolith afferent dynamics:

$$\frac{AFR(s)}{f(s)} = \frac{Bs + (B + C)A}{s + A} \qquad (11)$$

This model assumes that higher centers process the afferent response optimally to estimate the perceived specific force $\hat{f}$ as shown below.

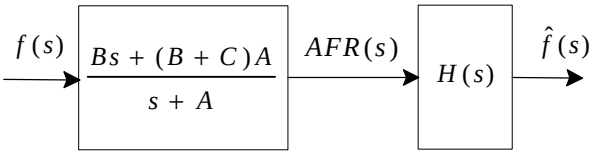

Combined Mechanical and Afferent Otolith Dynamics

Processing by Higher Centers

The steady-state optimal processor *H(s)* is then determined by solving the associated Wiener-Hopf equation, yielding a solution of the form

$$H(s) = M\frac{s + A}{(s + F)(s + G)} \qquad (12)$$

where *F*, *G*, and *M* are non-linear functions of a set of independent variables that include the parameters *A*, *B*, and *C* in Eqn. (11). With the form of *H(s)* determined, it can then be cascaded with the otolith and afferent dynamics to estimate the perceptual response:

$$\frac{\hat{f}}{f} = BM\frac{\left(s + \frac{(B + C)A}{B}\right)}{(s + F)(s + G)} \qquad (13)$$

which is equivalent to Eqn. (2).

Ormsby[2] noted that Fernandez, Goldberg, and Abend found an average steady-state change in afferent firing rate from the utricle due to a 1 g step to be 45 impulses per second (ips), resulting in the condition that $B + C = 45$. Setting Eqn. (13) equal to Eqn. (2) and including this constraint results in the following model for the afferent dynamic response:

$$\frac{AFR(s)}{f(s)} = 90\,\frac{s+0.1}{s+0.2} \tag{14}$$

This transfer function, when rearranged in terms of its time constants, becomes

$$\frac{AFR(s)}{f(s)} = 45\,\frac{10s+1}{5s+1} \tag{15}$$

Ormsby[2] noted the following about the model:

"The approach taken here can yield a model which accounts reasonably well for the available subjective data, the known physiological structure of the sensor and makes reasonable predictions concerning the afferent processes and the associated central processing."

Experimental Models of Afferent Dynamics

Fernandez and Goldberg[4] studied the discharge of peripheral otolith neurons in response to sinusoidal force variations in the squirrel monkey. Both regular and irregular units were measured, with a frequency analysis performed for each type of unit. The gain curves for the regular units were relatively flat, with a small phase lead at low frequencies and a larger phase lag at high frequencies. The irregular units showed a larger gain enhancement and phase lead at high frequencies. On average, there is an increase by a factor of 18 in gain enhancement in irregular units but only an increase of a factor of 2 for regular units. In both cases, a first-order lead operator cannot represent the resulting gain enhancement and phase lead. The average static sensitivity for both types of units is nearly identical, with reduced gains for the inhibitory response.

The frequency responses of regular and irregular units result in a transfer function of the form[4]

$$\frac{AFR(s)}{f(s)} = G_S\,\frac{1+k_A\tau_A s}{1+\tau_A s}\,\frac{1+k_\nu\left(\tau_\nu s\right)^{k_\nu}}{1+\tau_M s} = G_S\;H_A(s)\frac{H_\nu(s)}{H_M(s)} \tag{16}$$

In Eqn. (16), the term H_ν is a velocity-sensitive operator with a fractional exponent ($k_\nu < 1$) and provides most of the gain enhancement and phase lead found in both regular and irregular units. The value of k_ν reflects the effectiveness of the lead operator and is closely related to the slope of the gain curve. The term H_A is an adaptation operator that contributes to low frequency phase leads and gain increases from static or zero frequency to 0.006 Hz. The term H_M is a first-order lag operator that Fernandez and Goldberg[4] note may reflect the mechanics of otolith motion. This lag term accounts for the high frequency phase lags observed in regular units and for high frequency phase leads in irregular units being smaller than would be predicted solely by a fractional lead operator. The term G_S defines the static sensitivity in terms of afferent firing rate per unit of acceleration, i.e. ips/g.

The transfer function was estimated from a least square computer fit with τ_ν varied from 0 to 320 seconds in seven steps, with the remaining parameters estimated. The values for these parameters were obtained for $\tau_\nu = 40$ seconds (almost equal results were obtained for all values of τ_ν). The median parameters for both regular and irregular units for the excitatory response are given in Table 1.

Table 1. Median Parameters for Regular and Irregular Units[4].

Parameter	Regular Unit	Irregular Unit
k_ν	0.188	0.440
k_A	1.12	1.90
τ_A	69 sec	101 sec
τ_M	16 msec	9 msec
G_{DC}	25.6 ips / g	20.5 ips / g

Proposed Afferent Dynamics Model

Note that the gain terms for the Fernandez-Goldberg model from Table 1 are about one half that of the gain value used by Ormsby[2] to develop his model.

Due to the adaptation mechanism in the Fernandez-Goldberg models, these gains will require a long duration step input to be realized in steady state. Hosman[13] suggested a gain term of less magnitude than that used by Ormsby (G_{DC} = 33.3) that may provide an improved approximation to the Fernandez-Goldberg responses.

By using the long and lead time constants reported by Ormsby[2] in Eqn. (15), selecting the short time constant from the Fernandez-Goldberg[4] model, and including the gain suggested by Hosman, the following transfer function results for the afferent otolith dynamics:

$$\frac{AFR(s)}{f(s)} = 33.3\frac{(10s+1)}{(5s+1)(0.016s+1)} \qquad (17)$$

The frequency response of the proposed model in Eqn. (17) is compared to the frequency response of the Young-Meiry model of Eqn. (3) as shown in Figure 4. For comparison in Figure 4, both models use the gain K = 0.4 from the Young-Meiry model. Note that the gain and phase lag for the Young-Meiry model occurs at a much lower frequency as compared to the proposed model. This is due to the magnitude of the short time constant τ_2 for the Young-Meiry model being an order of magnitude larger than the value used in the proposed model. In the range of normal head movements from 0.1 to 1.0 Hz noted by Young[1], the gain for the proposed model remains constant with the phase close to zero degrees. In this frequency range the otolith functions as a specific force transducer.

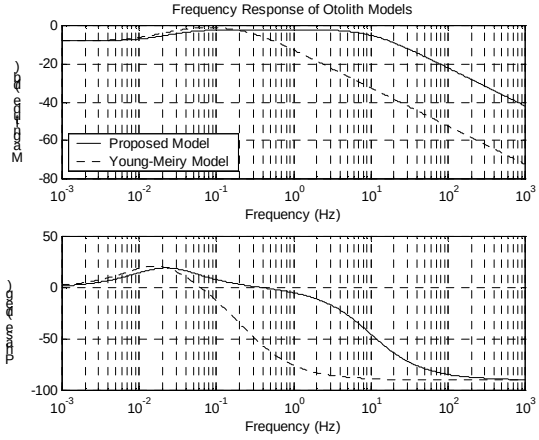

Figure 4. Frequency Response of Proposed and Young-Meiry Sensation Models.

Fractional Exponent Derivation

Because of the fractional exponent in the transfer function of Eqn. (16), an elementary solution to its response cannot be readily obtained. However, an approximate solution to the response can be derived through the application of fractional calculus[14].

By first substituting the regular unit parameters into Eqn. (16) and then implementing partial fraction expansion, Eqn. (16) becomes

$$H(s) = \frac{1792.056}{s+62.5} + 674.058\frac{s^{0.188}}{s+62.5} - \frac{0.044538}{s+0.0145} - 0.016752\frac{s^{0.188}}{s+0.0145} \qquad (18)$$

In Eqn. (18) there are two groups of two transfer functions. Each group is related to either the otolith mechanics ("fast") time constant τ_M or the adaptation ("slow") time constant τ_a, with one of the two transfer functions including an exponent that represents a fractional derivative. For the first group, the solution to the term without the fractional exponent can be easily obtained by taking the inverse Laplace transformation of the response:

$$L^{-1}\left(\frac{1}{s+62.5}\right) = e^{-62.5t} \qquad (19)$$

To derive a solution to the fractional exponent term, The inverse Laplace transformation is first obtained by applying fractional calculus:[14]

$$L^{-1}\left(\frac{s^{-\nu}}{s-a}\right) = E_t(\nu, a) \qquad (20)$$

where a = -62.5, ν = -0.188, and the term $E_t(\nu, a) = t^{\nu}e^{at}\gamma^*(\nu, at)$, with γ^* being the incomplete gamma function[14], a transcendental function that can be expressed as

$$\gamma^*(\nu, at) = t^{-at}\sum_{k=0}^{\infty}\frac{(at)^k}{\Gamma(\nu+k+1)} \qquad (21)$$

Substituting Eqn. (21) into Eqn. (20) will result in

$$L^{-1}\left(\frac{s^{-\nu}}{s-a}\right) = E_t(\nu, a) = t^{\nu}\sum_{k=0}^{\infty}\frac{(at)^k}{\Gamma(\nu+k+1)} \tag{22}$$

Eqn. (22) is an infinite series. For $\nu = 0$, Eqn. (22) will reduce to the Taylor series expansion of the exponential function:

$$E_t(0, a) = \sum_{k=0}^{\infty}\frac{(at)^k}{\Gamma(k+1)} = e^{at} \tag{23}$$

When ν is not equal to zero, $E_t(\nu, a)$ is a transcendental function that cannot be expressed by an elementary function, i.e. it can only be approximated. However, Eqn. (22) is not suitable for numeric computation because this series converges very slowly, especially when the magnitude of *a* is large (e.g. -62.5). The following derivation will result in an integral expression of the infinite series that can be adopted to compute $E_t(\nu, a)$. If we let $f(t) = E_t(\nu, a)$, then

$$f'(t) = t^{\nu-1}\sum_{k=0}^{\infty}\frac{(at)^k}{\Gamma(\nu+k)} \tag{24}$$

where $f(t)$ satisfies the first-order ordinary differential equation

$$f'(t) - a f(t) = t^{\nu-1}/\Gamma(\nu) \tag{25}$$

with the solution

$$f(t) = E_t(\nu, a) = \frac{e^{at}\int_0^t e^{-au}u^{\nu-1}du}{\Gamma(\nu)},\ \nu \geq 1 \tag{26}$$

Note that in Eqn. (26) the integral does not exist when ν - 1 is less than 0. To overcome this problem, we use the recursion formula[14]

$$\begin{aligned} E_t(\nu, a) &= \frac{t^{\nu}}{\Gamma(\nu+1)} + aE_t(\nu+1, a) \\ &= \frac{t^{\nu}}{\Gamma(\nu+1)} + \frac{at^{\nu+1}}{\Gamma(\nu+2)} + \frac{a^2e^{at}}{\Gamma(\nu+2)}E_t(\nu+2, a) \\ &= \frac{t^{\nu}}{\Gamma(\nu+1)} + \frac{at^{\nu+1}}{\Gamma(\nu+2)} + \frac{a^2e^{at}}{\Gamma(\nu+2)}\int_0^t e^{-au}u^{\nu+1}du \end{aligned} \tag{27}$$

Note that the integral in Eqn. (27) now exists since ν + 1 is greater than 0. Eqn. (27) can now be used to compute the responses of the two fractional exponent transfer functions given in Eqn. (18). For each of these transfer functions, three terms are computed. The first two terms are analytical functions, and the third includes an integral that requires an approximate solution. By using a series approximation, the integral *I(t)* in Eqn. (27) can be evaluated as

$$I(t) = t^{\nu+2}e^{-at}\left\{\sum_{j=0}^{N}C_j\int_0^1 e^{at(1-z)}(z-1)^j\,dz + O\left(\frac{1}{(-at)^{N+1}}\right)\right\} \tag{28}$$

where the constant C_j is equal to 1 for $j = 0$, $(\nu + 1)$ for $j = 1$, and $(\nu+1)\nu/2!$ for $j = 2$. By taking the inverse Laplace transformation of Eqn. (18) and applying Eqns. (27) and (28) to the transfer functions with fractional exponents results in the impulse response *h(t)*:

$$\begin{aligned} h(t) = {} & 1792.056e^{-62.5t} - 0.044538e^{-0.0145t} \\ & + 674.058\,E_t(-0.188, -62.5) \\ & - 0.016752\,E_t(-0.188, -0.0145) \end{aligned} \tag{29}$$

The response to a step input will now be considered. Given a system with the initial conditions $x = 0$ and $\dot{x} = 0$ when $t = 0$, and an arbitrary input *u(t)*, we look for a solution in the form

$$x(t) = \int_0^t h(x, \tau)u(\tau)d\tau \tag{30}$$

where $h(x, \tau)$ is Green's function, i.e. the system response to an impulse input. If we consider the response to a unit step, i.e. $u(\tau) = 1$ for t > 0, the response for a term without the fractional exponent is

$$\int_0^t e^{a\tau} d\tau = \frac{1}{a}\left(e^{at} - 1\right) \tag{31}$$

while the response for a term with the fractional exponent from Eqn. (29) is given by Miller and Ross[14] as

$$\int_0^t E_\tau\left(\nu, a\right) d\tau = E_t\left(\nu + 1, a\right) \tag{32}$$

and applying the recursion formula in Eqn. (27) gives

$$E_t\left(\nu + 1, a\right) = \frac{1}{a}\left(E_t\left(\nu, a\right) - \frac{t^\nu}{\Gamma\left(\nu + 1\right)} \right) \tag{33}$$

Applying Eqns. (31) and (33) to the impulse response given in Eqn. (29) and combining terms results in the regular unit response to a unit step:

$$\begin{aligned} x(t) &= 25.601 - 28.673e^{-62.5t} + 3.073e^{-0.014493t} \\ &\quad - 10.786E_t\left(-0.188, -62.5\right) \\ &\quad + 1.156E_t\left(-0.188, -0.014493\right) \\ &\quad + 9.629\frac{t^\nu}{\Gamma\left(\nu+1\right)} \end{aligned} \tag{34}$$

Similarly, the unit step response for the irregular unit can be derived:

$$\begin{aligned} x(t) &= 20.308 - 35.588e^{-111.1111t} + 18.280e^{-0.009901t} \\ &\quad - 86.063E_t\left(-0.44, -111.1111\right) \\ &\quad + 40.769E_t\left(-0.44, -0.009901\right) \\ &\quad + 45.294\frac{t^\nu}{\Gamma\left(\nu+1\right)} \end{aligned} \tag{35}$$

Comparisons of Model Responses

The response to a step input of 1 g (9.81 m/s^2) will now be examined for both the regular and irregular units. A series approximation of N = 2 will be used, and the responses will be evaluated at intervals of 0.025 seconds. The effect of the two fractional exponent lead terms from the otolith mechanics ("fast") and adaptation ("slow") time constants will be illustrated. Figure 5 shows the response for the regular units for 1 second. Note that the rise time is faster and the steady state response significantly increases due to the fast lead term, with a smaller but additional effect due to the slow lead term.

Figure 6 shows the response for the irregular units for 1 second. Note that both lead terms have a more significant effect on the response as compared to their effect on regular unit response. This is primarily due to the larger fractional exponent k_ν, and also due to the larger time constant τ_a and coefficient k_a in the adaptation operator. The rise time is significantly faster, with the response rapidly increasing to a peak overshoot over five times the value without the fast lead term. The inclusion of the fast lead term also results in the steady state response being nearly doubled. The addition of the slow lead term results in the overshoot increasing by an additional 50 per cent with additional steady state response.

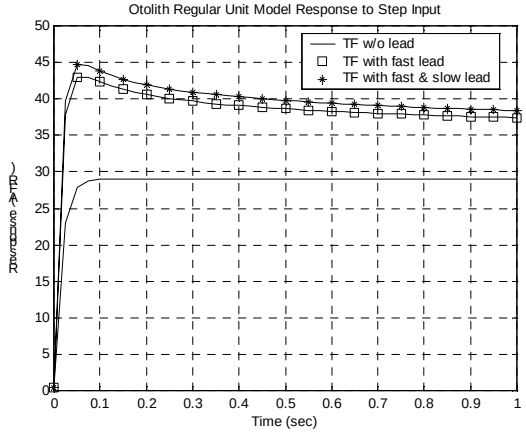

Figure 5. Regular Unit Response to Step Input.

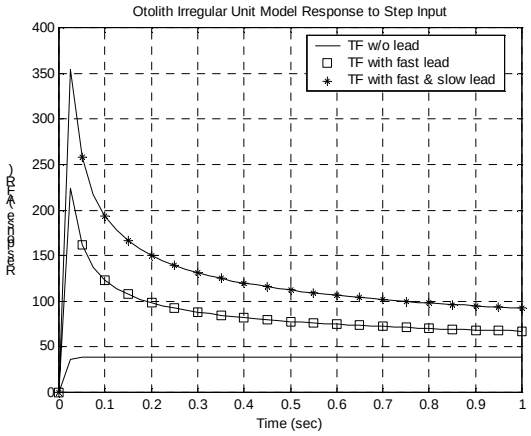

Figure 6. Irregular Unit Response to Step Input.

Figure 7 compares the step response for both the regular and irregular units (including both the fast and slow lead terms) to the response for the proposed model given in Eqn. (17). Note that the rise time for the proposed model is faster than the regular unit, but slower than the irregular unit. There is no large overshoot as observed with the irregular unit response. Figure 8 compares the responses for 30 seconds. Note that the steady state response for the proposed model is less than the irregular unit response but greater than the regular unit response, and approaches the regular unit response for the given time duration. Both the regular and irregular unit response will slowly approach their respective gain values, and beyond about 80 seconds the irregular unit response will decrease below that of the proposed model.

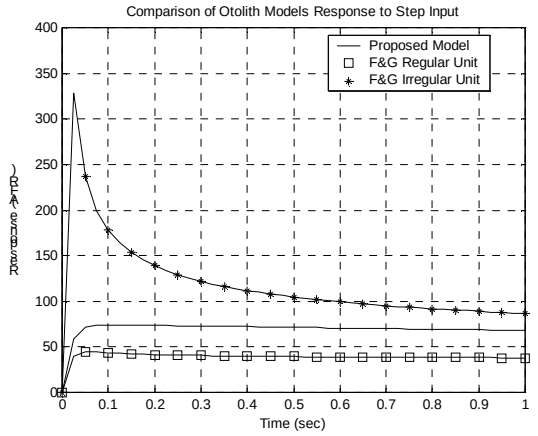

Figure 7. Proposed Model Response to Step Input for 1 second.

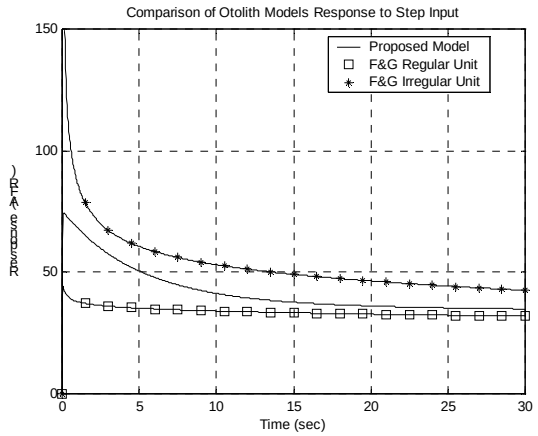

Figure 8. Proposed Model Response to Step Input for 30 seconds.

Physiological Interpretation

Modern theories of the operation of the otolith receptors are based on the assumption that the neural impulses are generated by the deflection of hairs in the sensory cells as a result of the otolith displacement. Specific force, produced by either linear acceleration or tilt, is first transformed into electrical impulses by the otolith-endolymph system. Then the otolith deflection is further transformed into electrical impulses by the mechano-neural transduction system consisting of sensory hair cells, afferent nerves, and efferent nerves.

Many researchers have shown that the otolith-endolymph system could be represented by an overdamped mass-spring-damper system. Grant and Best[11] reported that the magnitude of the long time constant τ_1 is considered correct by most investigators because the overall system (otolith organ, nervous transmission, central nervous system processing, and eye motion dynamics) could easily follow such a slow system. The value Grant and Best[11] obtain for the short time constant τ_2 is a three order of magnitude decrease in time constant as compared to the value obtained from the ocular torsion responses measured by Young and Meiry[8]. This value is also two orders of magnitude less than the value of τ_M Fernandez and Goldberg[4] attribute to the otolith dynamics. The dynamic response increases as the system transducer (otolith) is approached, thus allowing for dynamic losses in nervous system transmission and eye dynamics.

Young and Meiry[8] first noted that the origin of the lead term could be neurological, either in central processing of the otolith displacement signals or through the presence of two types of hair cells in the macula. One type of hair cell would respond to displacement and the other would respond to the rate of change of otolith displacement. These hair cells could produce the lead term if they were of the slowly adapting type postulated by several researchers. Fernandez and Goldberg[4] later show that the degree of sensitivity to the otolith velocity can be represented by different fractional exponents in the lead operator, i.e. irregular units are more velocity sensitive than regular units. They note that this difference in sensitivity may be due to discrepancies that are more noticeable with irregular units.

Fernandez and Goldberg[4] suggest that the difference between the expected otolith displacement

and afferent firing rate for both regular and irregular units may be attributed to the mechanical linkages between the sensory hair bundles and the gelatinous layer. They report that these sensory hair bundles are not rigidly embedded in the membrane, but are enclosed in a fluid-filled meshwork between the membrane and the sensory epithelium. Motion could be transferred to the hairs either by directly contacting the meshwork or indirect contact by viscous coupling with the fluid. They also note that the irregular units correspond to thick afferents that stimulate the Type I hair cells in the striola. Grant and Best[11] also suggest that for large tilt the gelatinous layer has a nonlinear stiffness that could also contribute to these differences as well.

Fernandez and Goldberg[4] suggest that later stages of the transduction process may also influence the afferent dynamics, in particular adaptation, noting the following:

"Lowenstein found, in the ray, that afferents can show adaptation when galvanic currents are applied. We have made similar observations in the squirrel monkey (unpublished observations) and have noted a correlation between the degree of adaptation shown by a particular afferent in its response to natural and electrical stimulation"

They note that these results show that a detailed comparison of the response to galvanic and natural stimulation may help in assessing the contributions made by the various transduction stages in the filtering process between the motion of the otolith and the discharge of the afferent.

Conclusions

A mathematical model of the otolith organs based on both analytical modeling and physiological experiments is proposed. This model consists of a second-order mass-spring-dashpot operator cascaded with a first-order lead operator. The mass-spring-dashpot operator represents the mechanics of otolith motion. The lead operator arises from the mechano-neural transduction system that in turn generates the afferent response.

The physiological experiments resulted in transfer functions for both regular and irregular units with a fractional exponent in the lead operator. This term reflects the sensitivity of hair cells to the rate of change of otolith displacement. By applying fractional calculus, transient responses to impulse and step inputs have been derived for both regular and irregular unit models. The solutions to these responses are both mathematically and computationally intensive, requiring several terms along with a series approximation of an integral for each of two lead components to compute the response at each time step.

Additional research in this area is needed to yield responses to more arbitrary inputs in addition to the impulse and step inputs. It is also suggested that a model could be developed that incorporates the dynamics of the fractional exponent lead operator from both the regular and irregular unit models. Such a model must be easy to implement in state space in a motion cueing algorithm and be computationally efficient so that the afferent response can be computed in real time.

Comparison of the transient response of the proposed model with the responses of the regular and irregular units clearly shows that a less complex model can generate a response that is a reasonable approximation between the regular and irregular units. This model has the same structure as the Meiry-Young model that is currently used in the development of the optimal algorithm[15], and can easily replace the former model. This revised otolith model will also be an integral part of a proposed motion cueing algorithm that incorporates human perception of motion into a non-linear optimal control structure.

References

[1] Young, L. H., Perception of the Body in Space: Mechanisms, Handbook of Physiology – The Nervous System III, Chapter 22, pp. 1023 – 1066.

[2] Ormsby, C. C., Model of Human Dynamic Orientation, Thesis, Massachusetts Institute of Technology, Cambridge, MA, January 1974.

[3] Howard, I. P., Chapter 11, The Vestibular System, pp. 11-1 – 11-30, in Handbook of Perception and Human Performance, Volume I, Sensory Processes and Perception, Boff, K. R., Kaufman, L., and Thomas, J. P, ed., John Wiley and Sons, Inc., New York , 1986.

[4] Fernandez, C. and Goldberg, J. M., Physiology of Peripheral Neurons Innervating Otolith Organs of the Squirrel Units, III: Response Dynamics. Journal of

Neurophysiology, v. 39, no. 5, September 1976, pp. 996 – 1008.
[5] Purves, Augustine, Fitzpatrick, Katz, LaMantia, & McNamara, Neuroscience, Sinauer Associates, Inc, Sunderland, MA, 1997.
[6] Fernandez , C. and Goldberg, J. M., Physiology of Peripheral Neurons Innervating Otolith Organs of the Squirrel Monkey, I: Response to Static Tilts and to Long-Duration Centrifugal Force., Journal of Neurophysiology, v. 39, no. 5, September 1976, pp. 970 – 983.
[7] Zacharias, G., "Motion Cue Models for Pilot-Vehicle Analysis", Defense Documentation Center, Defense Logistics Agency, AMRL-TR-78-2, May 1978.
[8] Young, L. R., and Meiry, J. L., "A Revised Dynamic Otolith Model", Aerospace Medicine, June, 1968, vol. 39, no. 6, pp. 606 – 608.
[9] Grant, J. W., Best, W.A., and LoNigro, R., Governing Equations of Motion for the Otolith Organs and their Response to a Step Change in Velocity of the Skull, Journal of Biomechanical Engineering, Transactions of the ASME, vol. 106, no. 4, Nov. 1984, pp. 302 – 308.
[10] Grant, J. W., Best, W. A., Mechanics of the Otolith Organ – Dynamic Response, Annals of Biomedical Engineering, vol. 14, 1986, pp. 241 – 256.
[11] Grant, W. and Best, W., Otolith-Organ Mechanics: Lumped Parameter Model and Dynamic Response, Aviation, Space, and Environmental Medicine, October, 1987, pp. 970 – 976.
[12] Grant, W. and Best, W., Viscoelastic Effects in Distributed Parameter Otolith Modeling, ASME Applied Mechanics Division Symposia Series, v. 84, 1987, pp. 299 – 302.
[13] Hosman, R. J., Pilot's Perception and Control of Aircraft Motions, Thesis, Delft University of Technology, The Netherlands, 1996.
[14] Miller and Ross, An Introduction to the Fractional Calculus and Fractional Differential Equations, John Wiley and Sons, Inc., New York, 1993.
[15] Telban, R. J., Cardullo, F. M., and Houck, J. A., Developments in Human Centered Cueing Algorithms for Control of Flight Simulator Motion Systems, AIAA Modeling and Simulation Technologies Conference, Portland, OR, August 9 – 11, 1999, pp. 463 – 473.